Fish & Shellfish Immunology 28 (2010) 862–871

Contents lists available at ScienceDirect

Fish & Shellfish Immunology

journal homepage: www.elsevier.com/locate/fsi

Antioxidant enzymes from the crab *Scylla paramamosain*: Gene cloning and gene/protein expression profiles against LPS challenge

Hai-Peng Liu [1], Fang-Yi Chen [1], Singaram Gopalakrishnan, Kun Qiao, Jun Bo, Ke-Jian Wang*

State Key Laboratory of Marine Environmental Science, College of Oceanography and Environmental Science, Xiamen University, Xiamen 361005, Fujian, PR China

ARTICLE INFO

Article history:
Received 18 November 2009
Received in revised form
27 January 2010
Accepted 3 February 2010
Available online 11 February 2010

Keywords:
Scylla paramamosain
Catalase (CAT)
Superoxide dismutase (SOD)
Lipopolysaccharide (LPS)

ABSTRACT

Recent studies revealed that antioxidant enzymes play important roles in antioxidant responses caused by metabolic process or pathogen invasion. Catalase is one of these key enzymes which has been characterized and highly conserved from invertebrates to vertebrates. In the present study, a full-length cDNA sequence of catalase was cloned from the hemocyte suppression subtractive hybridization library of the crab *Scylla paramamosain*. The *Sp*-catalase (*Sp*-CAT) cDNA sequence contained 2551 bp with an open reading frame of 1551 bp encoding 517 amino acid residues. The conserved catalytic active residues His-71, Asn-144 and Tyr-354 were predicted in the amino acid sequence of *Sp*-CAT. The deduced *Sp*-CAT protein had a calculated molecular mass of 59 kDa with an estimated isoelectric point of 6.4. Multiple alignment analysis revealed that the deduced amino acid sequence of *Sp*-CAT shared high identity (75.4%) with those of other species. The *Sp*-CAT mRNA transcripts were demonstrated in multiple tissues of normal *S. paramamosain*. After LPS challenge, the expression level of *Sp*-CAT gene was increased significantly in hemocyte at 3 and 6 h, and in hepatopancreas at 6 h, respectively, determined by quantitative real-time PCR. Furthermore, the activities of CAT and SOD were also measured in different tissues and serum after LPS challenge. The CAT activity was significantly increased at 3, 6, 24 and 48 h in hemocyte lysate, at 3 h in serum, and at 24 and 48 h in hepatopancreas after LPS challenge. In addition, the SOD activity was significantly induced at 3 and 6 h in hemocyte lysate, 3 and 12 h in serum, 12 and 48 h in hepatopancreas post LPS stimulation, indicating a tissue and time-dependent antioxidant response in the crab. Taken together, these data demonstrated that a strong antioxidant response occurred in the LPS-challenged crab, which might be involved in the protection of host against microbial infections.

© 2010 Elsevier Ltd. All rights reserved.

1. Introduction

In eukaryotes, the innate immune system is a critical means of host defense against microbial infections, especially for invertebrates lacking of adaptive immunity. One of these protective defenses is the generation of microbicidal reactive oxygen species (ROS) [1–3]. ROS could be constantly produced in response to both external and internal stimuli in aerobic organisms [4] and may play multiple functions in many biological processes [5]. Low levels of ROS have been shown to be involved in many biochemical processes like intracellular signaling in the cell differentiation and cell progression or the arrest of growth, apoptosis [6], immunity [7] and defense against microbial infection [8,9]. Whereas the high levels of ROS and reactive oxygen intermediates (ROI) may lead to cell damage [10]. Therefore, elimination or detoxification of residual ROS/ROI on time is critical for host to protect itself from damage. The antioxidant enzymatic system is then recruited for protecting the host from the toxic effects by the activated oxygen species [11,12]. These enzymes include catalase (CAT, EC 1.11.1.6), superoxide dismutase (SOD, EC1.15.1.1), glutathione reductase, glutathione peroxidase, glutareodoxin and thioredoxin reductase. Previous studies showed that a balance between the activities and the intracellular levels of these antioxidants was necessary for the survival of organisms and their health [13,14]. In animals, SOD detoxifies superoxide radicals by converting them to hydrogen peroxide and oxygen. Hydrogen peroxide is then detoxified by CAT and by glutathione peroxidase (GPX). CAT is a tetrameric oxidoreductase that catalyzes the conversion of two molecules of hydrogen peroxide to two molecules of water and one of oxygen. When injected intravenously with liposomes containing CAT and SOD, the rats exhibited increased survival of rates following the exposure to 100% oxygen [15]. Therefore, CAT is thought as a key enzyme of the antioxidant defense systems which can protect host cells by removing cytotoxic H_2O_2 [16,17].

* Corresponding author. Tel.: +86 592 2184658; fax: +86 592 2180655.
E-mail address: wkjian@xmu.edu.cn (K.-J. Wang).
[1] These authors made equal contributions.

1050-4648/$ – see front matter © 2010 Elsevier Ltd. All rights reserved.
doi:10.1016/j.fsi.2010.02.008

A number of studies on CAT enzyme activities or gene expression have been described from invertebrates to vertebrates including *Drosophila melanogaster* [11], *Chlamys farreri* [18], *Litopenaeus vannamei* [19], *Fenneropenaeus chinensis* [20], *Scylla paramamosain* [21], *Carcinus maenas* [22], *Macrobranchium malcolmsonii* [23], *Danio rerio* [24], *Mus musculus* [25], and *Homo sapiens* [26]. Importantly, recent investigations demonstrate that ROS-dependent immunity is critical to host survival in the *Drosophila* [27,28], the *Anopheles* [3], and the *Lymnaea* [29]. In crustaceans, it has been reported that the antioxidant enzymes like CAT and SOD participate in their innate immune defense against immune-stimulant challenges such as β-glucan and sulphated polysaccharide, white spot syndrome virus (WSSV), or Taura syndrome virus [30–35]. In contrast, little is known about the responses of antioxidant enzymes like CAT and SOD in farmed crabs after the challenge of immune-stimulant such as LPS, which is an important component of Gram-negative bacterium. In our previous study, a partial cDNA sequence of *Sp*-CAT gene was screened from the hemocyte subtractive suppression hybridization (SSH) library of the crab *S. paramamosain* and the transcript of *Sp*-CAT gene showed strong up-regulation after the LPS challenge [21]. Following the previous work, a full-length cDNA of *Sp*-CAT gene was then characterized and its tissue distribution was investigated in *S. paramamosain* in the present study. To reveal whether *Sp*-CAT gene really responded against immune-stimulant challenges as observed in other crustaceans, the expression profile in hemocyte and hepatopancreas after LPS challenge was determined using quantitative real-time PCR. In addition, the protein activities of CAT and SOD, which was also an important antioxidant enzyme gene identified previously from our SSH library [21], against LPS challenge were in parallel determined in different tissues of the crab *S. paramamosain*.

2. Materials and methods

2.1. Experimental animals

Live healthy female *S. paramamosain* (300 ± 50 g in weight) purchased from a local commercial crab farm in Xiamen, China, were acclimated at 25 ± 2 °C for one week before the experiments were carried out.

2.2. Determination of the full-length cDNA of Sp-CAT gene

To isolate the full-length *Sp*-CAT cDNA sequence of *S. paramamosain*, 5′-RACE and 3′-RACE were performed. Specific primers for *Sp*-CAT cDNA were designed according to the obtained partial cDNA sequence (Genbank no. FJ774660) from our previous study [21]. The RACE cDNA was prepared with an SMART RACE cDNA Amplification kit (Clontech, USA) according to the manufacturer's protocol and was used as template for PCR. The primers 5′-CAACACTCCCATCTTCTTCATCAGG-3′and 5′-TGTTGTTTCTGGACGCAGGGTGAT-3′ were used for 3′ RACE and 5′ RACE of *Sp*-CAT gene, respectively. PCR conditions were as follows: 94 °C for 1 min, 35 cycles of 94 °C for 40 s, 60 °C for 30 s and 72 °C for 2 min. The final extension was carried out at 72 °C for 7 min. The expected DNA fragment was eluted from agarose gel and ligated to pMD18-T vector (Takara). The ligation product was transformed into *Escherichia coli*. The recombinant clones harvesting the target gene were identified by bacterial-colony PCR as previously described [21]. The positive clones were sequenced in both directions and the resulting sequences were verified and subjected to Cluster analysis.

2.3. Establishment of a putative 3D-model structure of Sp-CAT protein

The establishment of putative 3D-model structure was performed with 3D-JIGSAW Protein Comparative Modeling Server (http://bmm.cancerresearchuk.org/~3djigsaw/) by comparing to human catalase as a Protein identifier (*PDB1F4S*).

2.4. The mRNA transcript distribution of Sp-CAT gene in the crab

Haemolymph of three healthy crabs (about 300 ± 50 g in weight per crab) was taken from the base of right chelate leg. Two millilitres of haemolymph per crab was individually collected into an equal volume of anti-coagulant solution (NaCl 510 mM; glucose 100 mM; citric acid 200 mM; Na-citrate 30 mM; EDTA-Na_2 10 mM; pH 7.3) [36] followed by centrifugation at 800 × g at 4 °C for 20 min. The resulting hemocyte pellet was used for total RNA isolation. Other tissues including brain, eyestalk, gills, heart, hepatopancreas, midgut gland, muscle, ovary, reproductive tract, stomach, subcuticular epithelia, and thoracic ganglion mass were also dissected and prepared for total RNA isolation. Total RNA was extracted from samples using Trizol reagent following the manufacturer's instructions and quantified with an Ultrospec 2100 pro spectrophotometer (Amersham Biosciences, Sweden). Five micrograms of total RNA for each tissue was separately reverse-transcribed in a final volume of 100 μl using a PrimeScript™ RT reagent kit (Perfect Real Time) (TaKaRa) following the manufacturer's instructions. Primers of 5′-CAACACTCCCATCTTCTTCATCAGG-3′ and 5′-TGTTGTTTCTGGACGCAGGGTGAT-3′ were used as forward and reverse primers, respectively. Real-time PCR was performed in a reaction mixture of 20 μl containing 0.5 ng of total transcribed cDNA, 5 pmol of each gene-specific primer and 10 μl of Power SYBR Green PCR Master Mix (Applied Biosystems, UK). The standard cycling conditions were 95 °C for 10 min, followed by 40 cycles of 95 °C for 15 s, 60 °C for 1 min. Data of raw relative quantification were calculated using 7500 system SDS software version 1.3.1.21 and the actin gene was employed as the internal standard.

2.5. The gene expression profile of Sp-CAT gene in hemocyte and hepatopancreas of the crab after LPS challenge

LPS from *E. coli* (L2880, Sigma, USA) was dissolved with modified crab saline solution (NaCl, 496 mM; KCl, 9.52 mM; $MgSO_4$, 12.8 mM; $CaCl_2$, 16.2 mM; $MgCl_2$,0.84 mM; $NaHCO_3$, 5.95 mM; HEPES, 20 mM; pH 7.4) [37] to be 5 mg ml^{-1} for animal challenge.

For the gene expression study, 15 crabs were injected with a dose of 0.5 mg kg^{-1} LPS and the other 15 individuals were injected with an equal volume of sterile saline solution as control treatments, respectively. The crabs for each group (3 crabs per group) were separately reared in individual tank under the same culture conditions. Meanwhile, three normal crabs were reared in an individual tank as a normal control group. Sampling was performed at different time intervals (3, 6, 12, 24 and 48 h) after LPS challenge. Haemolymph was collected as described above. Hemocyte pellets were preserved in Trizol reagent (Invitrogen) immediately for RNA extraction. Samples from the hepatopancreas were also separately collected from each individual animal and were individually frozen immediately in liquid nitrogen, then stored at −80 °C for later use. The total RNA isolation, real-time PCR quantification and data analysis were performed as described above.

2.6. Determination of antioxidant enzyme activities in the crab after LPS challenge

2.6.1. Samples preparation

The LPS challenge experiments were performed as described above. The samples were collected from each crab of the LPS challenged, saline injection and normal groups ($n = 3$) at different time points. Haemolymph collection and hemocyte preparation were performed as mentioned above. The hemocyte above was suspended in 100 mM sodium phosphate buffer (pH 7.0) containing 0.5 mM

EDTA and 1 mM phenylmethylsulfonyl fluoride (protease inhibitor) and subjected to cells disruption by sonication (20 kHz, 50 W, 3 × 20 s) in an ultrasonicator (Scientz JY92-II, Ning Bo Xinzi) and the resultant homogenates were centrifuged at 12,000 × g for 30 min at 4 °C. An aliquot of the resulting supernatant (hemocyte lysate) from each sample was used for the determination of CAT and SOD activity, respectively. For serum preparation, haemolymph was collected from individual crab in a pre-chilled Eppendorf tube and allowed to clot for 15 min at room temperature. The clot was disturbed with a clean glass rod and centrifuged at 500 × g for 10 min at room temperature. The resulting clear supernatant (serum) was used for all analyses. The protein concentrations were determined by Bradford method [38]. Tissue samples thus collected as mentioned above were homogenized (1:10 w/v) in 100 mM sodium phosphate buffer (pH 7.0) containing 0.5 mM EDTA and 1 mM phenylmethylsulfonyl fluoride and then centrifuged at 12,000 × *g* for 30 min at 4 °C, and the resulting supernatant was used for the determination of CAT and SOD activity, respectively.

2.6.2. CAT activity

The CAT activity was determined in different tissues/cells or serum according to the method of Sinha [39]. Shortly, dichromate in acetic acid was reduced to chromic acetate when heated in the presence of H_2O_2 with the formation of perchromic acid as an unstable intermediate. The reaction was allowed to continue for different periods of time and then terminated by the addition of dichromate-acetic acid mixture. The remaining H_2O_2 was determined by measuring the chromic acetate colorimetrically at OD_{570} nm. The CAT activity was expressed as μ mol of H_2O_2 consumed/min/mg protein.

2.6.3. SOD activity

The SOD activity was estimated by the method of Marklund and Marklund [40]. Briefly, the assay mixture contained 2 ml of 50 mM Tris–HCl buffer (pH 8.5), 0.5 ml of 2.6 mM pyrogallol and the sample extract. The rate of inhibition of pyrogallol auto-oxidation after the addition of enzyme extract was noted. The amount of enzyme required to give 50% inhibition of pyrogallol auto-oxidation was considered as one unit of enzyme activity. The enzyme activity was defined as Units/min/mg protein.

2.6.4. Statistical analysis

For all statistical data analysis, one-way analysis of variance (one-way ANOVA) followed by Student's *t*-test using SPSS 11.0 software was employed. Differences between saline control and LPS-challenged crabs were considered to be significant at $P < 0.05$. Results were interpreted as mean ± S.E. of three observations per group.

3. Results and discussion

Many Gram-negative bacteria like *Vibrios* are crab-pathogenic pathogens. Whereas, the knowledge of immune response against bacterial infection in farmed crabs is still limited. LPS is a well-known component of Gram-negative bacterium exhibiting strong immune stimulatory activity by inducing the release of proinflammatory cytokines from various target cells [41]. The present study was then focused on the antioxidant response of a CAT gene and a previously identified SOD gene [21] from the crab *S. paramamosain*, and the interaction between the CAT/SOD activities and their potential immune roles after LPS challenge was expected.

3.1. Determination of the full-length cDNA sequence of Sp-CAT gene

The 5′-RACE and 3′-RACE were employed to get the full cDNA sequence of *Sp*-CAT gene. It contained 2551 bp including 57 bp in the 5′ untranslated region (UTR), an open reading frame (ORF) of 1551 bp, and a 940 bp in the 3′-UTR including a stop codon (TGA), a putative polyadenylation consensus signal and a polyA tail. The ORF of *Sp*-CAT cDNA consisted of 517 amino acids. No signal peptide was predicted by SignalP (http://www.cbs.dtu.dk/services/SignalP/) in the N-terminus, suggesting that *Sp*-CAT protein was a non-secretory protein. The calculated molecular mass of the mature protein was 59 kDa with an estimated isoelectric point of 6.4. The full-length cDNA sequence and its deduced amino acid sequences were deposited in the NCBI GenBank under accession number of FJ774660 (updated with full cDNA sequence) (Fig. 1). Multiple sequences alignment showed that the *Sp*-CAT amino acid sequence exhibited overall high identity (75.4%) to members of the catalase family from other species including *Portunus trituberculatus* (ACI13850), *F. chinensis* (ABW82155), *Daphnia magna* (ACU81116), *D. melanogaster* (NP_536731), *Bombyx mori* (BAD38853), *Anopheles gambiae* (ABL09378), *D. rerio* (NP_570987), *M. musculus* (NP_033934), and *H. sapiens* (NP_001743) (Fig. 2). The three highly conserved catalytic amino acid residues (His-71, Asn-144 and Tyr-354 in the crab sequence) existed in all species compared here and were indicated by closed circles. The CAT proximal active site feature (FDRERIPERVVHAKGAGA) and the proximal heme-ligand signature sequence (RLFAYTDTH) were also highly conserved in the sequences analyzed. In addition, the predicated peroxysome targeting signal in the C-terminus was AKL which was the same to *F. chinensis* [20] but differing from the canonical signal found in human and mouse catalase (KAN), and one residue difference from that of mosquito and domestic silkworm catalase (ANL). This result implied that the crab *Sp*-CAT was likely to be a peroxisomal protein which is the case for most vertebrate and insect members of this family. By using immunoelectron microscopic analysis, previous study has indicated that the marine invertebrate CAT from the crustacean *C. maenas* and the mollusk *Mytilus galloprovincialis* were localized in the peroxisomes [22].

A crystal structure of crab CAT is not yet available, but it is likely that the catalytic site is much similar to other catalases based on their high identities to each other. The putative secondary structure was obtained by using the NPS@: Network Protein Sequence Analysis [42]. The total secondary structure content of crab CAT predicted by the NPS-algorithm was 28% of α-helix and 18% of β-sheet, which was similar to the structural contents of shrimp CAT (24% α-helix and 18% β-sheet) [19] and human CAT (25% α-helix and 14% β-sheet from structure *PDB1F4S*). The putative 3D-model structure of *Sp*-CAT protein was established by using the 3D-JIGSAW Protein Comparative Modeling Server (http://bmm.cancerresearchuk.org/~3djigsaw/) using human catalase (*PDB1F4S*) as a Protein identifier (Fig. 3).

3.2. Tissue distribution of Sp-CAT gene transcript in the crab

The presence of *Sp*-CAT mRNA in multiple tissues was determined by real-time PCR. As shown in Fig. 4, high expression was observed in hepatopancreas and midgut, followed by stomach. Relatively high expression was found in heart, muscle, thoracic ganglion mass, and eyestalk. Low expression was shown in brain, reproductive tract, ovary, gill, subcuticular epithelia and hemocyte. The hepatopancreas is a gland showing highly metabolic activity [43], and able to produce large amount of ROS [44]. Thus, the high expression of *Sp*-CAT gene in hepatopancreas might imply that it is likely to act as an important detoxification molecule in the crab.

3.3. Gene expression profile of Sp-CAT gene in hemocyte and hepatopancreas after LPS challenge determined by quantitative real-time PCR

To determine the transcript expression profile of *Sp*-CAT gene after LPS challenge, real-time PCR was employed. Because of the important roles of hemocyte and hepatopancreas for generation of

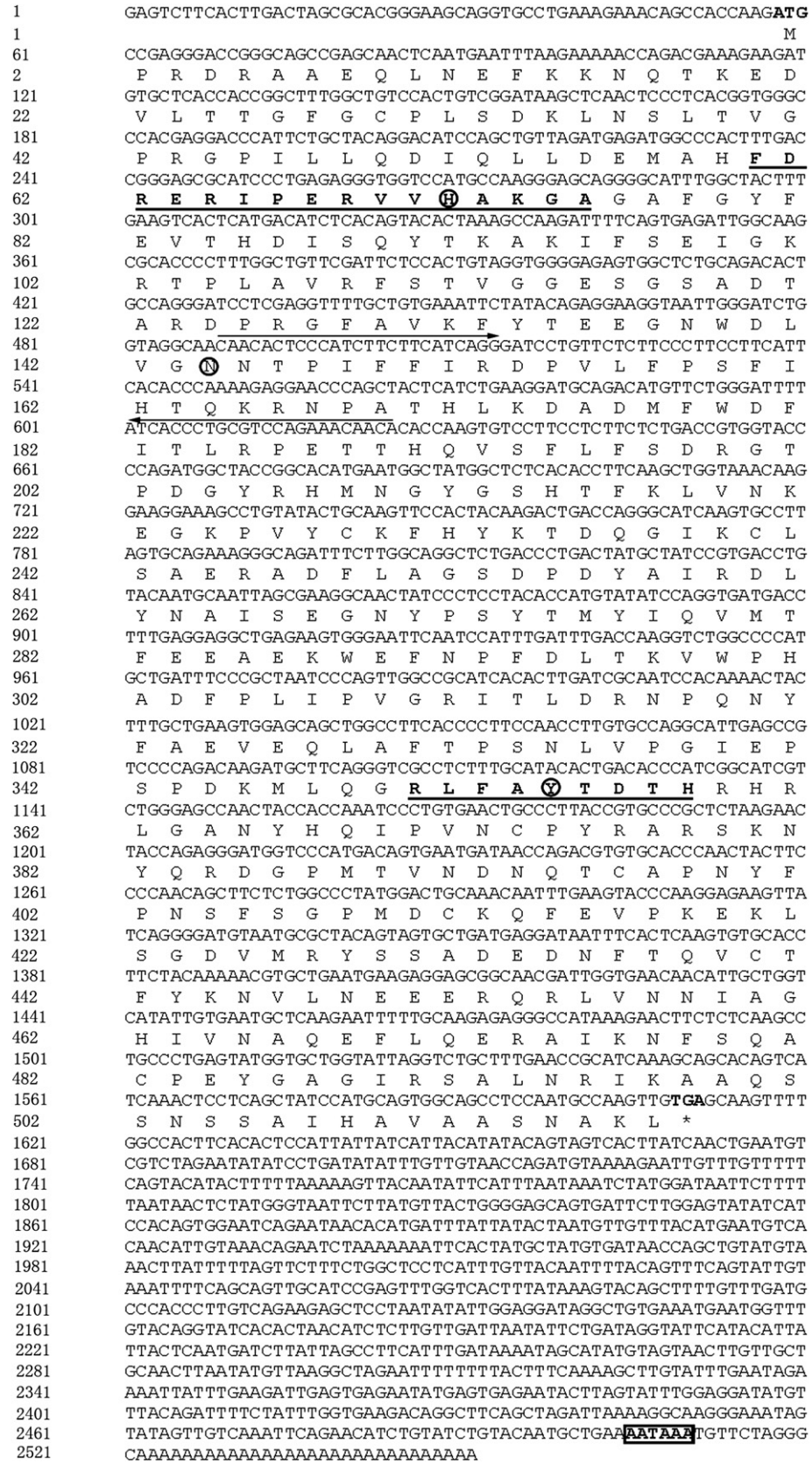

Fig. 1. Complementary DNA and predicted amino acid sequences of *Sp*-CAT gene. The polyadenylation signal (AATAAA) was in bold and boxed. The start coden (ATG) and stop codon (TGA) were in bold. The three catalytic amino acid residues (His-71, Asn-144 and Tyr-354) were shown in bold and circled. The catalase proximal active site feature (FDRERIPERVVHAKGAGA) and the proximal heme-ligand signature sequence (RLFAYTDTH) were indicated in bold and underlined. Primers for 5′-, 3′-RACE and analysis of gene differential expression sites were shown with arrows (5′–3′) (GenBank accession number FJ774660).

Fig. 2. Multiple sequences alignment of the deduced amino acid residues of the *Sp*-CAT with catalases from selected species: *Portunus trituberculatus* (ACI13850), *Fenneropenaeus chinensis* (ABW82155), *D. magna* (ACU81116), *Drosophila melanogaster* (NP_536731), *B. mori* (BAD38853), *Anopheles gambiae* (ABL09378), *Danio rerio* (NP_570987), *M. musculus* (NP_033934), and *H. sapiens* (NP_001743). The three conserved catalytic amino acid residues from all species analyzed were shown with closed circles. And the catalase proximal active site feature (FDRERIPERVVHAKGAGA) and proximal heme-ligand signature sequence (RLFAYTDTH) were boxed.

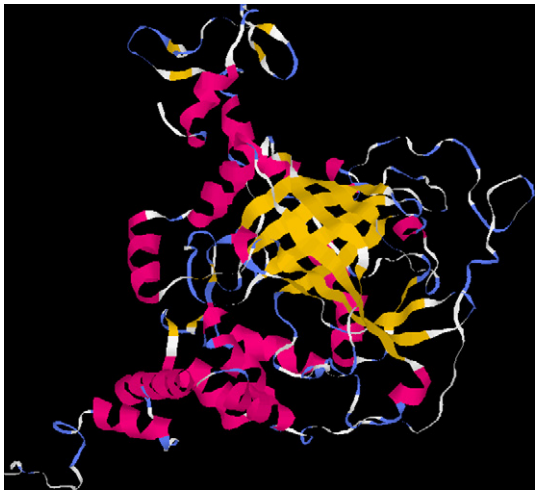

Fig. 3. A putative 3D-model structure of *Sp*-CAT protein. The model was established by using the 3D-JIGSAW Protein Comparative Modeling Server (http://bmm.cancerresearchuk.org/~3djigsaw/).

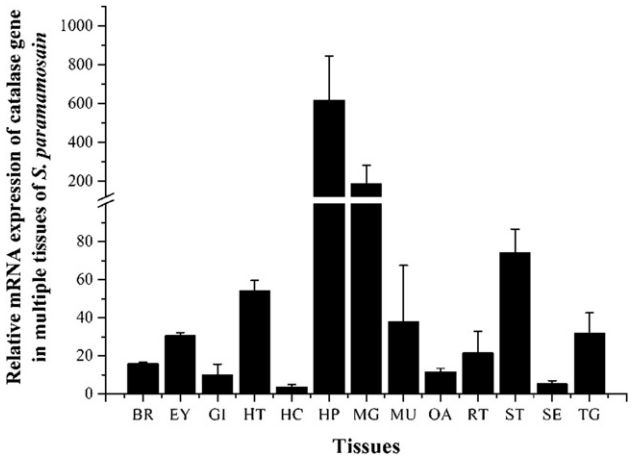

Fig. 4. Distribution of the *Sp*-CAT gene transcript in different tissues by real-time PCR. Tissues analyzed: brain (BR); eyestalk (EY); gills (GI); heart (HT); hemocyte (HC); hepatopancreas (HP); midgut gland (MG); muscle (MU); ovary (OA); reproductive tract (RT); stomach (ST); subcuticular epithelia (SE); thoracic ganglion mass (TG). This experiment was performed for three times and the data demonstrated means of triplicates. Bars indicated mean ± S.E. ($n = 3$).

immune defense molecules in crustaceans, the differential expression patterns of *Sp*-CAT gene in hemocyte and hepatopancreas during the time course of LPS challenge were analyzed. After LPS challenge, the *Sp*-CAT gene transcript was significantly expressed in hemocyte at 3 h (8.2-fold, $P < 0.01$) and maintained high expression till 6 h (12.1-fold, $P < 0.01$) (Fig. 5A). The level of *Sp*-CAT transcripts was higher in LPS treated animals compared to controls treatment at 24 h clearly confirming the SSH results (about 2-fold increase) in our previous study, in which the expression of *Sp*-CAT gene was increased in crab hemocyte post LPS challenge [21]. In contrast, the *Sp*-CAT gene showed a reduced expression for both control and LPS treated animals at 3 h compared to that of untreated animals in hepatopancreas. After that, the *Sp*-CAT mRNA transcripts in the LPS-challenged animals were increased to the normal level at 6 h with a significant difference (7.1-fold) when compared to those of saline injected group. The *Sp*-CAT transcripts showed lower expression again in the LPS treated animals from 12 h till the end of the experiments when compared to the normal crabs (Fig. 5B). These data together suggested that the gene expression pattern of *Sp*-CAT in the hepatopancreas was different from that in the hemocyte of the crab with LPS challenge.

3.4. Antioxidant enzyme activities in the crab after LPS challenge

3.4.1. CAT activity

After stimulation of LPS, the CAT activity showed variations in different tissues tested in the crab. The significant induction of CAT activity was observed at 3 (1.5-fold), 6 (1.3-fold), 24 (1.29-fold) and 48 h (1.3-fold), but not at 12 h, in the hemocyte lysate of the LPS-challenged crabs when compared to that of saline injected group (Fig. 6A). This activity profile perfectly matched with the induced expression profile of *Sp*-CAT gene against LPS stimulation (Fig. 5A). Whereas for serum post LPS challenge, the CAT activity was significantly induced only at 3 h (1.4-fold) (Fig. 6B), indicating that the induction pattern of CAT activity in serum was different from that in hemocyte lysate. This result clearly confirmed our previous study, in which the mRNA transcript of *Sp*-CAT gene showed strong up-regulation in a crab hemocyte SSH library after the LPS stimulation. However, this was not the case for hepatopancreas, where the CAT enzyme activity showed a delayed significant increase at 24 h in comparison with its gene expression (significant increase at 6 h). Besides, the CAT activity showed significant increase at 24 (5.7-fold) and 48 h (3.9-fold), but not other time points tested in the hepatopancreas, after LPS challenge (Fig. 6C). This variation was also

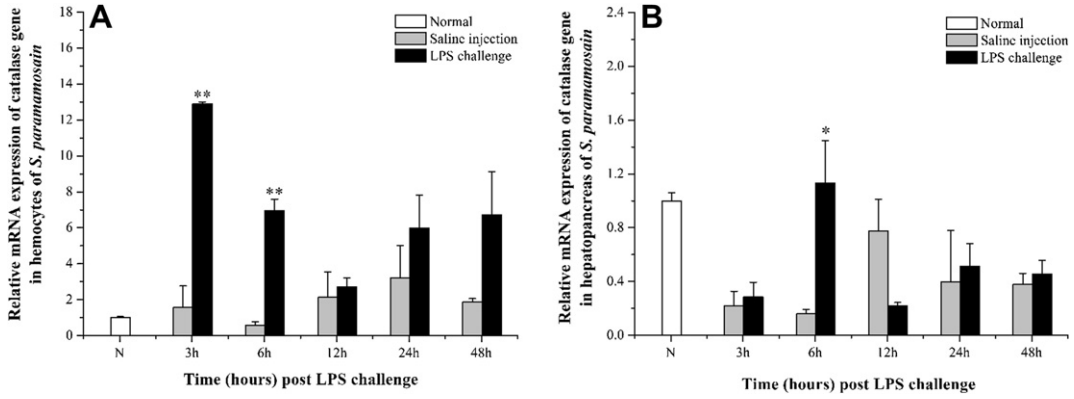

Fig. 5. The expression profile of *Sp*-CAT mRNA in hemocyte (Fig. 5A) and hepatopancreas (Fig. 5B) post LPS challenge by real-time PCR. The sampling was performed at 3, 6, 12, 24 and 48 h after LPS challenge. The significant difference of *Sp*-CAT transcripts between LPS-challenged group and control group was indicated with asterisks (**: $P < 0.01$, *: $P < 0.05$). The data demonstrated means of triplicates. Bars indicated mean ± S.E. ($n = 3$).

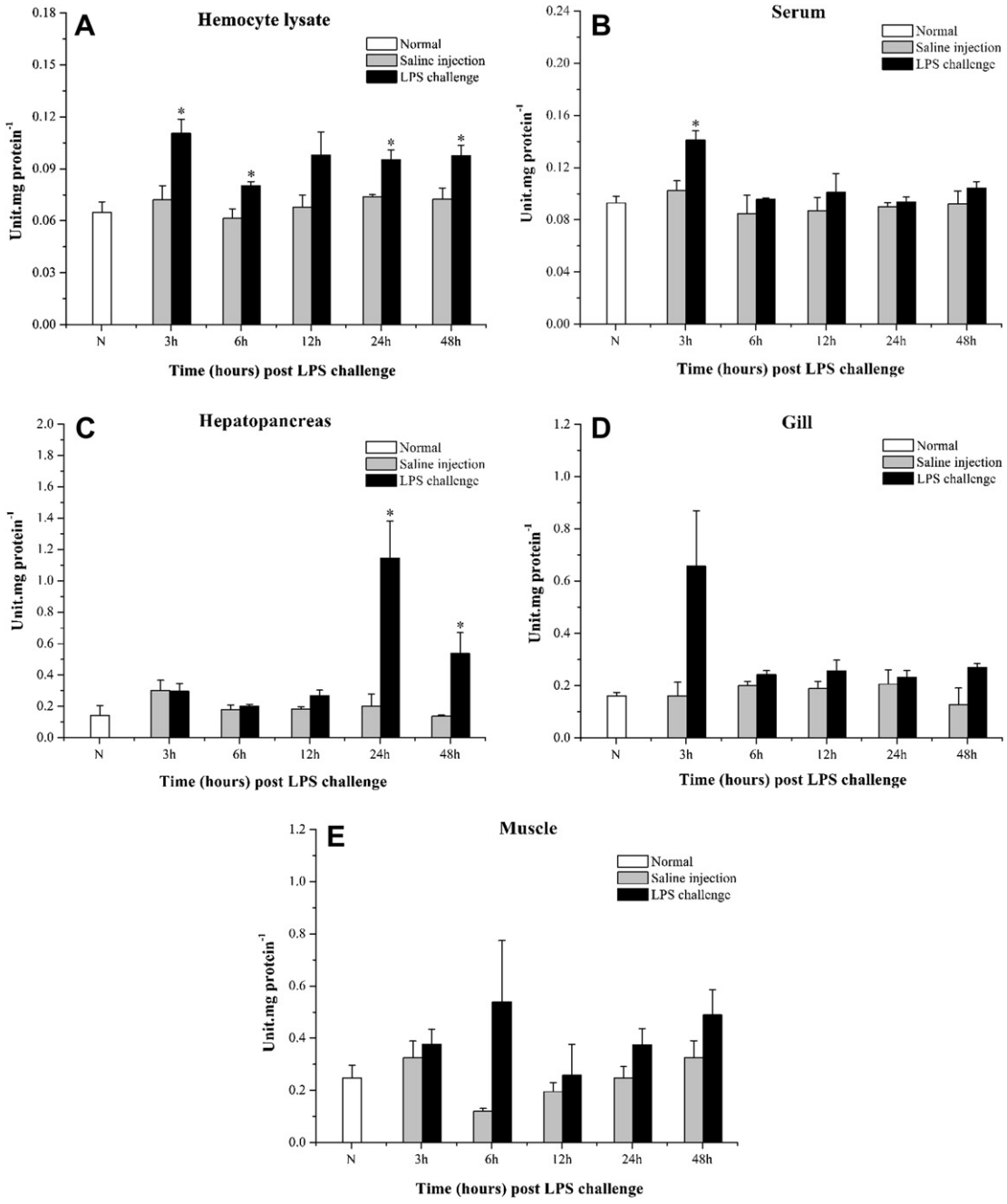

Fig. 6. CAT activity in different tissues after LPS challenge. The sampling was performed from hemocyte lysate, serum, hepatopancrease, gill and muscle at 3, 6, 12, 24 and 48 h after LPS challenge. The CAT activity for hemocyte lysate, serum, hepatopancreas, gill and muscle was illustrated in A, B, C, D, and E, accordingly. The significant difference of CAT activity between LPS-challenged group and control group was indicated with asterisks (*: $P < 0.05$). The data demonstrated means of triplicates. Bars indicated mean ± S.E. ($n = 3$).

observed in other crustaceans like shrimps, in which the expression level of CAT showed similar variations during early infection stages against a WSSV challenge [20]. The induced higher CAT activity was also acquired at 3 h in the crab gills after LPS challenge (Fig. 6D). Similarly, the enhanced CAT activity occurred in the muscles at 6 h post LPS stimulation compared to that of saline injected crabs (Fig. 6E). In addition, the CAT activity was also compared among different tissues/cells examined. For instance, the CAT activity was found strongly higher in the hepatopancreas than in the ovary, hemocyte, gills and muscle at 24 and 48 h after LPS challenge in our study (data not shown). In contrast, the CAT activity was more induced in the gills than in the ovary, hemocyte, muscle, and hepatopancreas at 3 h post LPS challenge. Taken together, the increased *Sp*-CAT expression and CAT activity after LPS challenge suggested an acute strong antioxidant response occurred in the crab hemocyte and other different tissues, indicating that *Sp*-CAT might act as an important acute defense molecule under stress of immuno-stimulant challenge or microbial infection.

3.4.2. SOD activity

SOD is an important enzyme that detoxifies toxic superoxide anion radicals and its activity has been taken as an important parameter usually measured under antioxidant response. In our previous study, the mRNA transcript of SOD has been found to be increased in the crab hemocyte against LPS challenge [21]. To further verify if the SOD

enzyme activity was correspondingly induced by LPS challenge, we then measured the SOD activity in this study. The specific activity profile of SOD enzyme was demonstrated in Fig. 7. It was observed that a significant induction of SOD activity occurred at 3 (2.1-fold) and 6 h (2.3-fold) in the hemocyte lysate post LPS challenge (Fig. 7A), which was strongly correlated to *Sp*-SOD gene expression profile as previously observed [21]. Meanwhile, a significant induction of SOD activity was also shown in the crab serum at 3 (1.5-fold) and 12 (1.6-fold) post LPS challenge (Fig. 7B), which exhibited a similar expression pattern to *Sp*-SOD gene in the hemocyte in our previous study [21]. In addition, the SOD activity was significantly induced at 12 h (1.3-fold) and 48 h (3.9-fold) when compared to that of saline injected animals, but no direct correlation existed between the SOD enzyme activity and the *Sp*-SOD gene expression level in the hepatopancreas of crabs with LPS challenge (Fig. 7C) [21]. This result indicated the complicated regulation of the antioxidant response in the hepatopancreas in a crustacean. Besides, a highly induced SOD enzyme activity was also observed in the gills and muscles at 3 h (Fig. 7D) and 48 h (Fig. 7E), respectively, after LPS challenge (but not in the ovary, data not shown). Besides, a relative high induction of SOD activity showed up in the gills at 3 h post LPS stimulation when compared to the hemocyte, muscle, ovary and hepatopancreas (data not shown). Together with the CAT expression features described above, these results indicated that the crab gills exhibited a relatively low-threshold response to the LPS challenge, which was similar to that of Spiny cheek crayfish investigated under different environmental conditions [45]. CAT enzyme is an important antioxidant component sharing the same function with glutathione peroxidase (GSH-Px) for

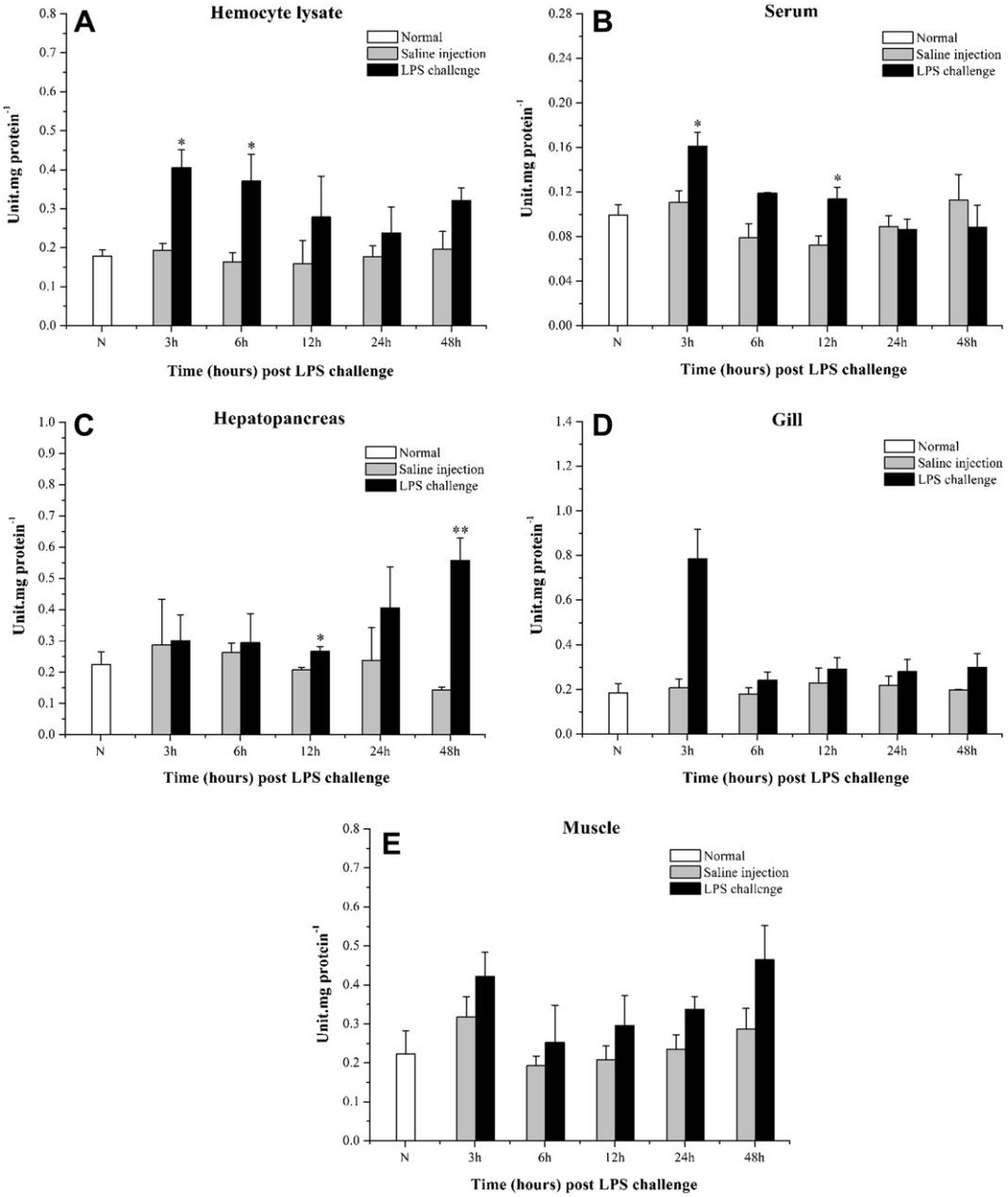

Fig. 7. SOD activity in different tissues after LPS challenge. The sampling was performed from hemocyte lysate, serum, hepatopancrease, gill and muscle at 3, 6, 12, 24 and 48 h after LPS challenge. The SOD activity for hemocyte lysate, serum, hepatopancreas, gill and muscle was illustrated in A, B, C, D, and E, accordingly. The significant difference of SOD activity between LPS-challenged group and control group was indicated with asterisks (**: $P < 0.01$, *: $P < 0.05$). The data demonstrated means of triplicates. Bars indicated mean ± S.E. ($n = 3$).

working primarily to degrade H_2O_2 to H_2O. Organic peroxides are the preferred substrate for GSH-Px in the presence of low H_2O_2 concentrations, but not at high level of H_2O_2, which are catalyzed by CAT [46]. Previous study has found that CAT plays a relatively more important role in detoxification in invertebrates than vertebrates [47]. Generally, any significant increase in SOD activity is accompanied by a comparable enhancement in CAT and/or GSH-Px activities [48]. Similar tendency was also found in our study. The high level of SOD activity was followed by the increased CAT activity accordingly in the hemocyte, serum, hepatopancreas and gill after LPS challenge. Taken together, our data revealed that the antioxidant enzyme activities like CAT/SOD varied in different tissues/cells against the LPS stress, suggesting that the enzyme activity along with their gene expression profile was tissue-specific as well as time-dependent under stress conditions.

3.4.3. Remarks and summary

A balanced activity of antioxidant components is needed for the homeostasis of ROS and the redox state [45]. To achieve this balance, anti-oxidative components must be coordinated by correlative changes with other antioxidant enzymes [49]. The ROS scavenging and the antioxidant defense system therefore play important roles in maintaining normal cellular physiology, dealing with diseases and enhancing immunity. Recent investigations strongly suggest that the ROS detoxification system plays important roles in host-microbe interactions. For instance, the *Plasmodium*-refractory *A. gambiae* strain exhibited increased stable levels of ROS, which favored parasite killing in the midgut. Meanwhile, the CAT was likely to promote parasite killing by encapsulation [50]. The ROS was also shown to modulate *A. gambiae* immunity, in which a local reduction of detoxification of hydrogen peroxide in the midgut, contributing to restrict *Plasmodium* infection via a lytic mechanism, was involved in responses to *P. berghei* [3]. In *Drosophila*, the antioxidant system was required for host protection against gut infection. The dynamics between infection-induced de novo ROS generation and efficient removing by immune-regulated catalase were essential biological process for its innate immunity [28]. Strong evidence suggested that pathogenic bacteria, like *Helicobacter pylori*, could induce ROS synthesis directly in the gastric epithelial cells of patients and result in DNA damage and apoptosis [51–53]. Besides, ROS was also involved in relatively common inflammatory diseases of the gastrointestinal tract like inflammatory bowel diseases [54,55]. Those results together indicate that fine redox balancing is one of the most important events involved in host-parasite as well as host–microbe interaction during mucosal infection.

In invertebrates, the role of the antioxidant defense system is much more important, because phagocytosis involving a highly ROS and ROI producer response is a key line of defense against invading microorganisms due to their lack of adaptive immunity [56,57]. However, the generation of high levels of ROS and ROI must be restricted and transient to avoid tissue damage. Many catalases and their genes from various species have been reported [58] and the numbers are in growing, whereas the marine invertebrate catalases are just recognized. It has been reported that the CAT/SOD activity or their gene expression increases parallel to immuno-stimulant challenge or pathogen infections in crustaceans [21,30,33–35,59]. To our best knowledge, there is no report so far for any protection test against microbe invasion under the condition of enhanced CAT/SOD activities in crustaceans, which hence needs to be further investigated in the future. In conclusion, the insightful information generated in this study will benefit further studies for evaluating the potential functions of CAT/SOD gene expression and their antioxidant activities against microbial infection commonly found in crab farming and/or the polluted environments.

Acknowledgements

This work was supported by a grant (40676083) from National Natural Science Foundation of China (NSFC), a grant (2007AA091406) from the National High Technology Research and Development Program of China (863 Program) and a grant from the Minjiang Scholars Program to K. J. Wang (2009); and a grant (2009J05084) from Natural Science Foundation of Fujian Province China (NSFC-FPC).

References

[1] Nakano H, Nakajima A, Sakon-Komazawa S, Piao JH, Xue X, Okumura K. Reactive oxygen species mediate crosstalk between NF-kappaB and JNK. Cell Death Differ 2006;13(5):730–7.
[2] Kohchi C, Inagawa H, Nishizawa T, Soma G. ROS and innate immunity. Anticancer Res 2009;29(3):817–21.
[3] Molina-Cruz A, DeJong RJ, Charles B, Gupta L, Kumar S, Jaramillo-Gutierrez G, et al. Reactive oxygen species modulate *Anopheles gambiae* immunity against bacteria and Plasmodium. J Biol Chem 2008;283(6):3217–23.
[4] Mates JM, Perez-Gomez C, Nunez de Castro I. Antioxidant enzymes and human diseases. Clin Biochem 1999;32(8):595–603.
[5] Lambeth JD. NOX enzymes and the biology of reactive oxygen. Nat Rev Immunol 2004;4(3):181–9.
[6] Ghosh J, Myers CE. Inhibition of arachidonate 5-lipoxygenase triggers massive apoptosis in human prostate cancer cells. Proc Natl Acad Sci U S A 1998;95(22):13182–7.
[7] Yin GY, Yin YF, He XF. Effect of zhuchun pill on immunity and endocrine function of elderly with kidney-yang deficiency. Zhongguo Zhong Xi Yi Jie He Za Zhi 1995;15(10):601–3.
[8] Bae YS, Kang SW, Seo MS, Baines IC, Tekle E, Chock PB, et al. Epidermal growth factor (EGF)-induced generation of hydrogen peroxide. Role in EGF receptor-mediated tyrosine phosphorylation. J Biol Chem 1997;272(1):217–21.
[9] Lee YJ, Galoforo SS, Berns CM, Chen JC, Davis BH, Sim JE, et al. Glucose deprivation-induced cytotoxicity and alterations in mitogen-activated protein kinase activation are mediated by oxidative stress in multidrug-resistant human breast carcinoma cells. J Biol Chem 1998;273(9):5294–9.
[10] Griswold CM, Matthews AL, Bewley KE, Mahaffey JW. Molecular characterization and rescue of acatalasemic mutants of *Drosophila melanogaster*. Genetics 1993;134(3):781–8.
[11] Mackay WJ, Bewley GC. The genetics of catalase in *Drosophila melanogaster*: isolation and characterization of acatalasemic mutants. Genetics 1989;122(3):643–52.
[12] Parkes TL, Hilliker AJ, Phillips JP. Genetic and biochemical analysis of glutathione-S-transferase in the oxygen defense system of *Drosophila melanogaster*. Genome 1993;36(6):1007–14.
[13] Mao GD, Thomas PD, Lopaschuk GD, Poznansky MJ. Superoxide dismutase (SOD)-catalase conjugates. Role of hydrogen peroxide and the Fenton reaction in SOD toxicity. J Biol Chem 1993;268(1):416–20.
[14] Sohal RS, Agarwal A, Agarwal S, Orr WC. Simultaneous overexpression of copper- and zinc-containing superoxide dismutase and catalase retards age-related oxidative damage and increases metabolic potential in *Drosophila melanogaster*. J Biol Chem 1995;270(26):15671–4.
[15] Turrens JF, Crapo JD, Freeman BA. Protection against oxygen toxicity by intravenous injection of liposome-entrapped catalase and superoxide dismutase. J Clin Invest 1984;73(1):87–95.
[16] Bai J, Rodriguez AM, Melendez JA, Cederbaum AI. Overexpression of catalase in cytosolic or mitochondrial compartment protects HepG2 cells against oxidative injury. J Biol Chem 1999;274(37):26217–24.
[17] Bai J, Cederbaum AI. Catalase protects HepG2 cells from apoptosis induced by DNA-damaging agents by accelerating the degradation of p53. J Biol Chem 2003;278(7):4660–7.
[18] Li C, Ni D, Song L, Zhao J, Zhang H, Li L, et al. Molecular cloning and characterization of a catalase gene from Zhikong scallop *Chlamys farreri*. Fish Shellfish Immunol 2008;24(1):26–34.
[19] Tavares-Sanchez OL, Gomez-Anduro GA, Felipe-Ortega X, Islas-Osuna MA, Sotelo-Mundo RR, Barillas-Mury C, et al. Catalase from the white shrimp Penaeus (*Litopenaeus*) *vannamei*: molecular cloning and protein detection. Comp Biochem Physiol B Biochem Mol Biol 2004;138(4):331–7.
[20] Zhang Q, Li F, Zhang X, Dong B, Zhang J, Xie Y, et al. cDNA cloning, characterization and expression analysis of the antioxidant enzyme gene, catalase, of Chinese shrimp *Fenneropenaeus chinensis*. Fish Shellfish Immunol 2008;24(5):584–91.
[21] Chen FY, Liu HP BJ, Ren HL, Wang KJ. Identification of genes differentially expressed in hemocytes of *Scylla paramamosain* in response to lipopolysaccharide. Fish Shellfish Immunol 2010;28:167–77.
[22] Orbea A, Fahimi HD, Cajaraville MP. Immunolocalization of four antioxidant enzymes in digestive glands of mollusks and crustaceans and fish liver. Histochem Cell Biol 2000;114(5):393–404.
[23] Arun S, Thirumurugan R, Visakan R, Balamurugan S, Arunachalam V, Subramanian P. Optimal analytical conditions for catalase in fresh water prawn, *Macrobrachium malcolmsonii*. Biotech Histochem 2003;78(1):1–4.

[24] Ken CF, Lin CT, Wu JL, Shaw JF. Cloning and expression of a cDNA coding for catalase from zebrafish (*Danio rerio*). J Agric Food Chem 2000;48(6):2092–6.
[25] Shaffer JB, Sutton RB, Bewley GC. Isolation of a cDNA clone for murine catalase and analysis of an acatalasemic mutant. J Biol Chem 1987;262(27):12908–11.
[26] Korneluk RG, Quan F, Lewis WH, Guise KS, Willard HF, Holmes MT, et al. Isolation of human fibroblast catalase cDNA clones. Sequence of clones derived from spliced and unspliced mRNA. J Biol Chem 1984;259 (22):13819–23.
[27] Ha EM, Oh CT, Bae YS, Lee WJ. A direct role for dual oxidase in *Drosophila* gut immunity. Science 2005;310(5749):847–50.
[28] Ha EM, Oh CT, Ryu JH, Bae YS, Kang SW, Jang IH, et al. An antioxidant system required for host protection against gut infection in *Drosophila*. Dev Cell 2005;8(1):125–32.
[29] Zelck UE, Janje B, Schneider O. Superoxide dismutase expression and H_2O_2 production by hemocytes of the trematode intermediate host *Lymnaea stagnalis* (Gastropoda). Dev Comp Immunol 2005;29(4):305–14.
[30] Campa-Cordova AI, Hernandez-Saavedra NY, De Philippis R, Ascencio F. Generation of superoxide anion and SOD activity in haemocytes and muscle of American white shrimp (*Litopenaeus vannamei*) as a response to beta-glucan and sulphated polysaccharide. Fish Shellfish Immunol 2002;12(4):353–66.
[31] Mohankumar K, Ramasamy P. White spot syndrome virus infection decreases the activity of antioxidant enzymes in *Fenneropenaeus indicus*. Virus Res 2006;115(1):69–75.
[32] Mathew S, Kumar KA, Anandan R, Viswanathan Nair PG, Devadasan K. Changes in tissue defence system in white spot syndrome virus (WSSV) infected *Penaeus monodon*. Comp Biochem Physiol C Toxicol Pharmacol 2007;145(3):315–20.
[33] Chongsatja PO, Bourchookarn A, Lo CF, Thongboonkerd V, Krittanai C. Proteomic analysis of differentially expressed proteins in *Penaeus vannamei* hemocytes upon Taura syndrome virus infection. Proteomics 2007;7(19):3592–601.
[34] Ji PF, Yao CL, Wang ZY. Immune response and gene expression in shrimp (*Litopenaeus vannamei*) hemocytes and hepatopancreas against some pathogen-associated molecular patterns. Fish Shellfish Immunol 2009;27(4):563–70.
[35] Munoz M, Cedeno R, Rodriguez J, van der Knaap W, Mialhe E, Bachere E. Measurement of reactive oxygen intermediate production in haemocyte of the penaid shrimp (*Penaeus vannamei*). Aquaculture 2000;191:89–107.
[36] Söderhäll K, Smith VJ. Separation of the haemocyte populations of *Carcinus maenas* and other marine decapods, and prophenoloxidase distribution. Dev Comp Immunol 1983;7(2):229–39.
[37] Cui Z, Liu H, Lo TS, Chu KH. Inhibitory effects of the androgenic gland on ovarian development in the mud crab *Scylla paramamosain*. Comp Biochem Physiol A Mol Integr Physiol 2005;140(3):343–8.
[38] Bradford M. A rapid and sensitive method for the quantification of protein-dye binding. Anal Biochem 1976;72:248–54.
[39] Sinha AK. Colorimetric assay of catalase. Anal Biochem 1972;47(2):389–94.
[40] Marklund S, Marklund G. Involvement of superoxide radicals in the auto oxidation of pyrogallol and a convenient assay for superoxide pyrogallol and a convenient assay for superoxide dismutase. Eur J Biochem 1974;47:469–74.
[41] Raetz CR, Whitfield C. Lipopolysaccharide endotoxins. Annu Rev Biochem 2002;71:635–700.
[42] Combet C, Blanchet C, Geourjon C, Deléage G. NPS@: network protein sequence analysis. TIBS 2000;25(3(291)):147–50.
[43] Mourente G. In vitro metabolism of 14C-polyunsaturated fatty acids in midgut gland and ovary cells from *Penaeus kerathurus* forskal at the beginning of sexual maturation. Comp Biochem Physiol B 1996;115:255–66.
[44] Arun S, Subramanian P. Antioxidant enzymes in fresh water prawn *Macrobrachium malcolmsonii* during embryonic and larval development. Comp Biochem Physiol B 1998;121:273–7.
[45] Borkovic SS, Pavlovic SZ, Kovacevic TB, Stajn AS, Petrovic VM, Saicic ZS. Antioxidant defence enzyme activities in hepatopancreas, gills and muscle of Spiny cheek crayfish (*Orconectes limosus*) from the River Danube. Comp Biochem Physiol C Toxicol Pharmacol 2008;147(1):122–8.
[46] Yu BP. Cellular defenses against damage from reactive oxygen species. Physiol Rev 1994;74(1):139–62.
[47] Livingstone DR, Lips F, Martinez PG, Pipe RK. Antioxidant enzymes in the digestive gland of the common mussel (*Mytilus edulis*). Mar Biol 1992;112: 265–76.
[48] Warner HR. Superoxide dismutase, aging, and degenerative disease. Free Radic Biol Med 1994;17(3):249–58.
[49] Pavlovic SZ, Belic D, Blagojevic DP, Radojicic RM, Zikic RV, Saicic ZS, et al. Seasonal variations of cytosolic antioxidant enzyme activities in the liver and white muscle of thinlip gray mullet (*Lizaramada Risso*) from the Adriatic Sea. Cryo Letters 2004;25(4):273–85.
[50] Kumar S, Christophides GK, Cantera R, Charles B, Han YS, Meister S, et al. The role of reactive oxygen species on *Plasmodium melanotic* encapsulation in *Anopheles gambiae*. Proc Natl Acad Sci U S A 2003;100(24):14139–44.
[51] Ernst PB, Gold BD. The disease spectrum of *Helicobacter pylori*: the immunopathogenesis of gastroduodenal ulcer and gastric cancer. Annu Rev Microbiol 2000;54:615–40.
[52] Obst B, Wagner S, Sewing KF, Beil W. *Helicobacter pylori* causes DNA damage in gastric epithelial cells. Carcinogenesis 2000;21(6):1111–5.
[53] O'Rourke EJ, Chevalier C, Pinto AV, Thiberge JM, Ielpi L, Labigne A, et al. Pathogen DNA as target for host-generated oxidative stress: role for repair of bacterial DNA damage in *Helicobacter pylori* colonization. Proc Natl Acad Sci U S A 2003;100(5):2789–94.
[54] Krieglstein CF, Cerwinka WH, Laroux FS, Salter JW, Russell JM, Schuermann G, et al. Regulation of murine intestinal inflammation by reactive metabolites of oxygen and nitrogen: divergent roles of superoxide and nitric oxide. J Exp Med 2001;194(9):1207–18.
[55] Pavlick KP, Laroux FS, Fuseler J, Wolf RE, Gray L, Hoffman J, et al. Role of reactive metabolites of oxygen and nitrogen in inflammatory bowel disease. Free Radic Biol Med 2002;33(3):311–22.
[56] Johansson MW, Holmblad T, Thörnqvist PO, Cammarata M, Parrinello N, Söderhäll K. A cell-surface superoxide dismutase is a binding protein for peroxinectin, a cell-adhesive peroxidase in crayfish. J Cell Sci 1999;112 (Pt 6):917–25.
[57] Cerenius L, Lee BL, Söderhäll K. The proPO-system: pros and cons for its role in invertebrate immunity. Trends Immunol 2008;29(6):263–71.
[58] Klotz MG, Klassen GR, Loewen PC. Phylogenetic relationships among prokaryotic and eukaryotic catalases. Mol Biol Evol 1997;14(9): 951–8.
[59] Dong C, Zhao J, Song L, Wang L, Qiu L, Zheng P, et al. The immune responses in Chinese mitten crab *Eriocheir sinensis* challenged with double-stranded RNA. Fish Shellfish Immunol 2009;26(3):438–42.